Journal of Structural Geology, Vol. 10, No. 7, pp. 701 to 705, 1988
Printed in Great Britain

0191-8141/88 $03.00 + 0.00

Universal stage measurements and transmission electron microscope observations of fractured plagioclase

DARIA MONICA AGUE

Department of Geology and Geophysics, University of California at Berkeley, Berkeley, CA 94720, U.S.A.

(*Received* 22 *December* 1987; *accepted in revised form* 16 *June* 1988)

Abstract—At low to moderate temperatures of deformation, fracturing of plagioclase is common. The mechanism of fracturing is generally thought to be either a dislocation assisted process with fractures typically exhibiting some crystallographic regularity or a process of breaking along cleavage planes without the involvement of dislocations. In this study, naturally fractured plagioclase from granodiorites and a gabbro deformed at high strain rates are examined with the transmission electron microscope (TEM) to identify structures at that scale. In addition, fracture orientations are determined with the Universal stage.

Some fractures observed in thin section occur parallel to (001) but many are not so simple but are confined to the [112], [1$\bar{1}$2], [101], [$\bar{1}$01] zones. At the TEM scale, dislocation walls or arrays are common in plagioclase. They also occupy the [101], [$\bar{1}$01], [112], [1$\bar{1}$2] zones. Microcracks form when dislocations are pinned in these arrays or when a free dislocation interacts with dislocations within a dislocation wall. In this way, large-scale fractures which develop inherit their crystallographic orientation from the dislocation wall.

INTRODUCTION

BRITTLE deformation of plagioclase takes place through fracturing along specific crystallographic planes, commonly along cleavage planes such as (010) and (001). Most fractures confined to individual crystals occur on low index planes (Brown & Macaudiere 1984). The crystallographic regularity of these intracrystalline fractures suggest that dislocations may be involved in their formation (Mitra 1978, Brown & Macaudiere 1984). However, fracture may occur by breaking along cleavage planes without involving dislocations (Tullis & Yund 1987).

Models of crack nucleation have been proposed for metals (Stroh 1957, Cottrell 1958, Li 1961) and probably apply to minerals. In general, all models require a limited amount of dislocation glide prior to fracturing. Dislocations may coalesce along their glide planes to form a microcrack, or a dislocation wall may act as a plane of weakness along which a microcrack can develop. These microcracks, which inherit a crystallographic orientation from the dislocation microstructure, act as nucleation sites for the intracrystalline fractures. In this study, fractured plagioclase from naturally deformed rocks is examined to establish the relationship between dislocation microstructures observed at the transmission electron microscope (TEM) scale and intracrystalline fractures observed at both the optical and TEM scales.

SAMPLE DESCRIPTIONS

Fractured plagioclase from a weakly and a strongly deformed (mylonitic) granodiorite and a moderately deformed gabbro were chosen for study. The granodiorites are part of the Santa Rosa Mylonite Zone of southern California. The gabbro is from the Musgrave Ranges located in Central Australia. Fracturing in the gabbro took place following a high temperature (700–800°C; Mirams 1964) ductile phase of deformation. Intracrystalline fractures in plagioclase (An_{48-52}) occur in 30% of the grains and commonly overprint deformation bands and deformation twins (Fig. 1a).

In the granodiorites, deformation took place at temperatures of 500–600°C (Theodore 1970). The weakly deformed granodiorite contains euhedral plagioclase (An_{35-40}) that ranges in size from 0.1 to 4 mm. Fractures occur in 10% of the grains, often near inclusions within the large crystals (Fig. 1b). The strongly deformed granodiorite (mylonite) contains plagioclase which is compositionally similar to that in the weakly deformed grandiorite with a slightly smaller average grain size (1.3 mm). Most feldspars in the mylonite are highly fractured and fragmented. Parts of entire crystals can sometimes be recognized (Fig. 1c).

FRACTURE ORIENTATIONS

The Universal stage was used to determine the orientation of the principal axes of the optical indicatrix and the orientation of twin and cleavage planes. All optically determined data were used to reconstruct the true crystal orientation by rotating the indicatrix axes in stereographic projection and matching them and the cleavage/twin planes with the migration curves of Burri *et al.* (1967). Placing the rotated optical data and rotated measured fracture planes on the curves allows a determination of the crystallographic orientations of the fractures.

The orientations of intracrystalline fractures with small but visible offsets were determined for plagioclase in the three rocks. (001) fractures are most common in the grandiorites (Fig. 3). (110) and ($\bar{1}$10) fractures are common in plagioclase from the granodiorites and the gabbro. Often fractures do not occur on simple crystal-

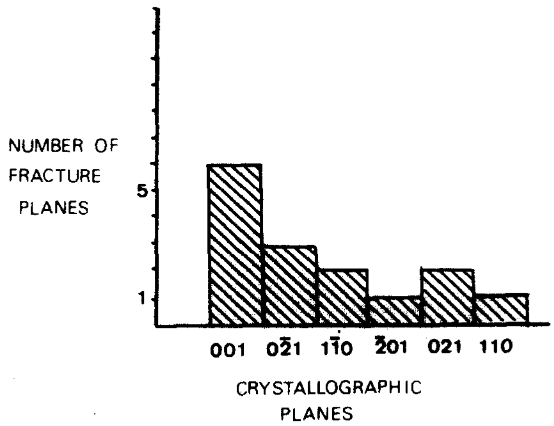

Fig. 3. Histogram of fracture orientations in plagioclase from the weakly deformed granodiorite measured with the Universal stage.

lographic planes and instead occupy the [112], $[1\bar{1}2]$, [101], $[\bar{1}01]$ zones (Fig. 4a & b).

TEM OBSERVATIONS

Selected feldspar crystals removed from thin section were ion-milled until perforated. The thin regions were examined with a JEOL JEM-100C transmission electron microscope (TEM) operating at 100 kV. All diffraction patterns for plagioclase are indexed based on the albite unit cell (c = 0.7 nm).

Various grains with small-scale fractures were examined with the TEM. At the TEM scale, grains contain visible fractures, but these fractures are not often preserved since ion milling will preferentially remove material from these regions. Trace analysis was applied to the limited number of fractures which were observed. At least two traces were used to identify the plane on which the fractures occur. Those measured occupy the [112] zone and spread out into the [101] and $[1\bar{1}2]$ zones (Fig. 4c).

In addition to fractures, isolated dislocation walls or arrays are common in plagioclase from the granodiorites and less common but present in the gabbro (Fig. 2b). These dislocation walls contain an evenly spaced set of dislocations. Other free dislocations, outside of the dislocation wall, often interact with dislocations in the wall (Fig. 2c). In these regions, the regular dislocation spacing may be disrupted and a small microcrack parallel to the wall may form (Fig. 2e). Dislocation walls have various orientations within a single grain, but they commonly intersect only in the strongly deformed granodiorite. Where they intersect, fine-grained micas may be present within a small crack (Fig. 2a). In grains with abundant dislocation walls, particularly those from the mylonite, the dislocation walls may join to enclose a region in the crystal, forming a small 'grain' with angular boundaries within the large crystal (Fig. 2d). Microcracks are observed crossing pre-existing features such as twins in some grains (Fig. 2f).

To determine the crystallographic orientation of the dislocation walls, trace analysis using several different

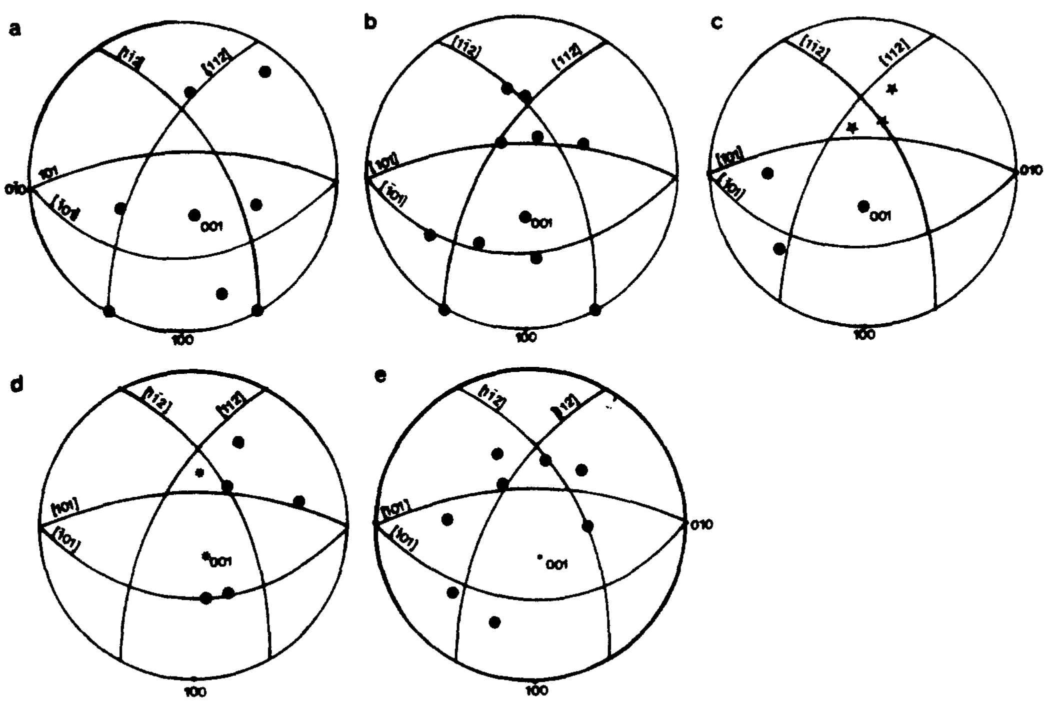

Fig. 4. Stereographic projections of poles to: (a) fractures in plagioclase from the granodiorites determined from Universal stage; (b) fractures in plagioclase from the gabbro determined from Universal stage; (c) fractures in the granodiorites (solid circles) and the gabbro (stars) as determined from their traces; (d) orientation of dislocation arrays/walls determined from trace analysis (TEM) for plagioclase from the weakly deformed granodiorite (solid circles) and the gabbro (asterisk); (e) orientations of dislocation walls/arrays determined from trace analysis (TEM) for plagioclase from the strongly deformed granodiorite. The [101], $[\bar{1}01]$, [112] and $(1\bar{1}2)$ zones and the (001) and (010) planes are plotted. $(\bar{1}11)$ lies at the intersection of $[1\bar{1}2]$ and [101] and $(\bar{1}\bar{1}1)$ lies at the intersection of [112] and [101]. The number of data points on each projection approximates the number of measurements made.

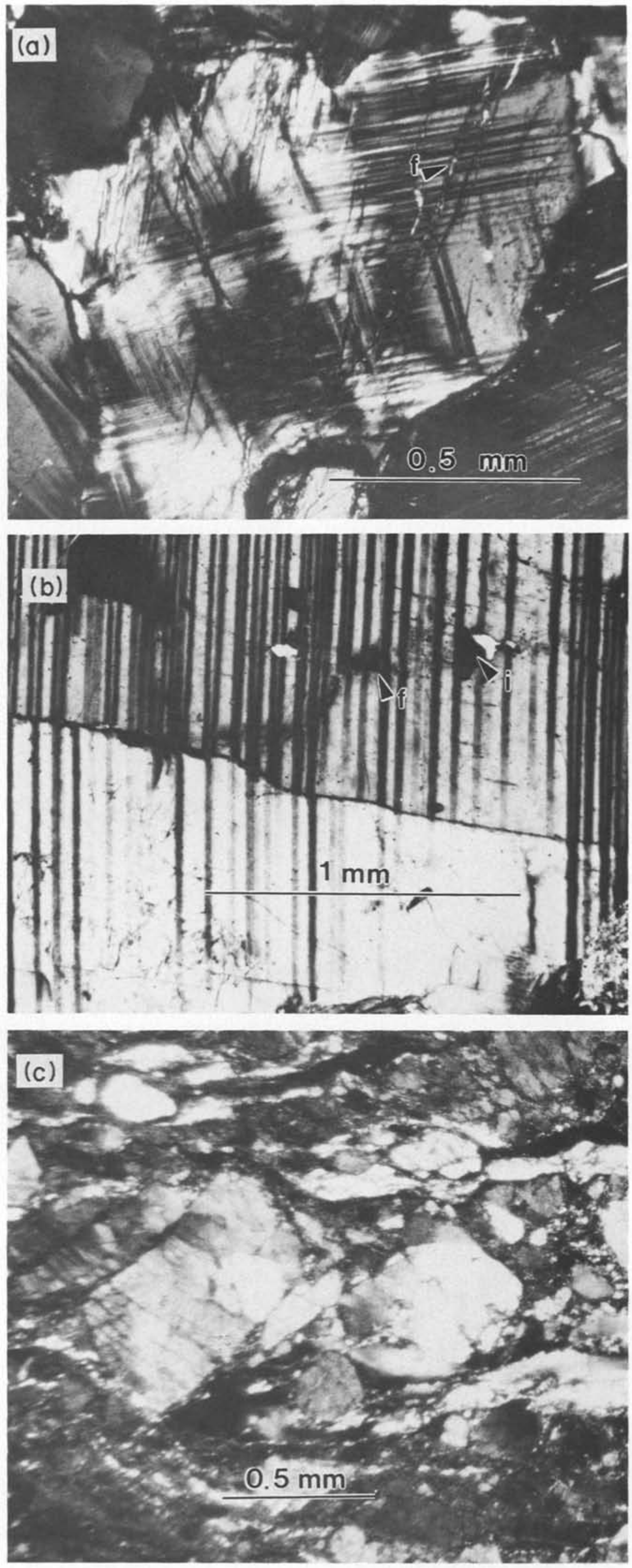

Fig. 1. (a) Optical photomicrograph (crossed-polarizers) of plagioclase from the deformed gabbro. Fractures (labelled f) typically cross-cut pre-existing features such as deformation twins or deformation bands (b) Optical photomicrograph (crossed-polarizers) of intracrystalline fractures, f, near an inclusion (i) in plagioclase from the weakly deformed granodiorite, (c) Optical photomicrograph (crossed-polarizers) of fragmented plagioclase from the strongly deformed granodiorite.

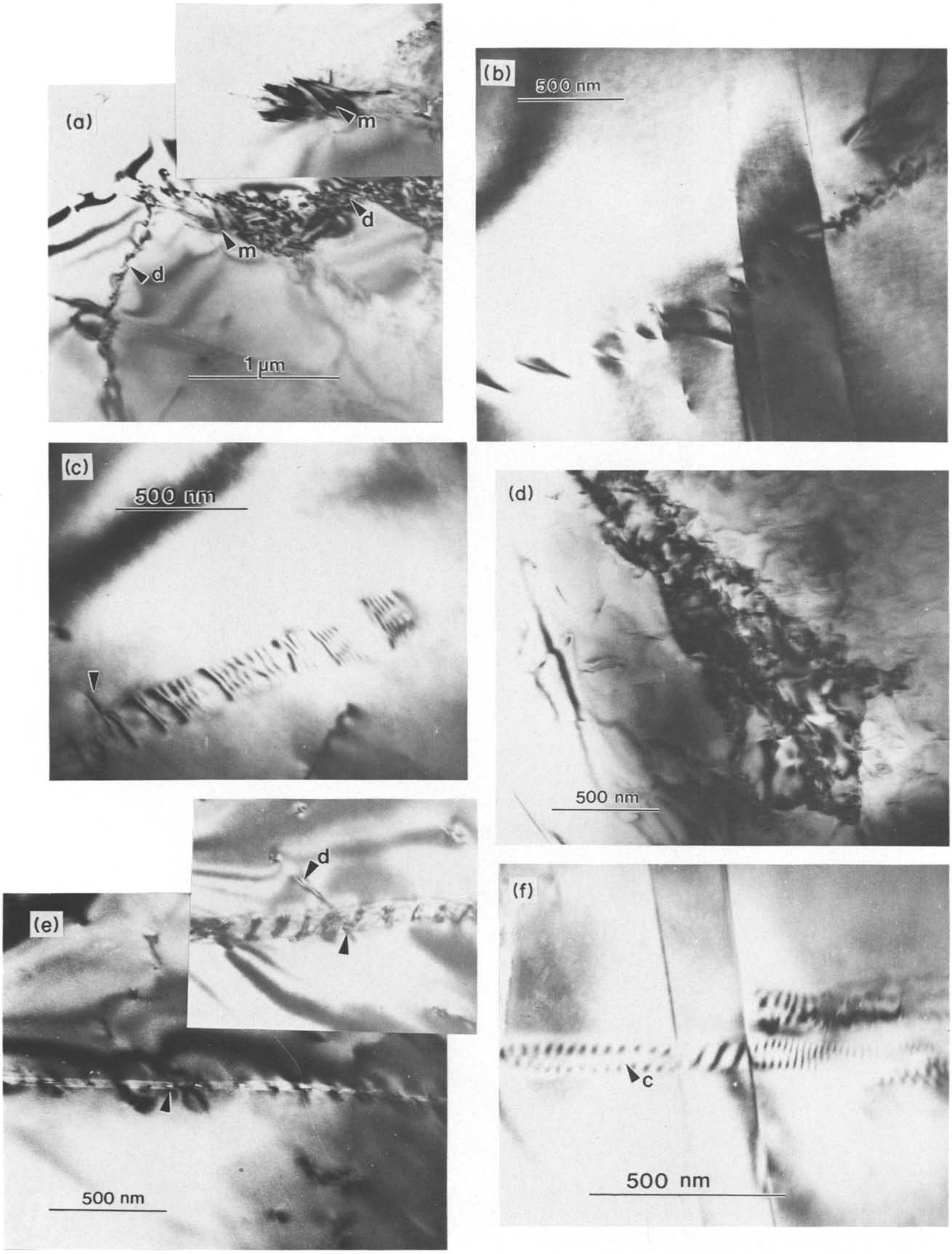

Fig. 2. Transmission electron microscope brightfield photographs. (a) Micas (seen clearly in the insert, labelled m) are sometimes observed at the intersection of dislocation arrays (d) where microcracks are produced. (b) A dislocation array in the weakly deformed granodiorite crosses a pre-existing twin. (c) A free dislocation (arrow) interacts with dislocations in an array. (d) Dislocation arrays can coalesce to enclose a 'sub-grain' within the host. The sub-grain exhibits different contrast from the host. (e) Microcracks (arrow) form along the dislocation wall where a free dislocation interacts with the wall. Insert of the same region (near the arrow) observed under different diffracting conditions showing the free dislocation (d) interacting with the dislocation wall. (f) Openings/microcracks (c) are observed across dislocation arrays (compare with b).

orientations was applied to the walls observed. The data points were used to reconstruct the plane and the poles to these planes are plotted in stereographic projection (Fig. 4). The dislocation wall orientations cluster about the $(\bar{1}11)$ and $(\bar{1}\bar{1}1)$ planes near the intersections of the [112], $[1\bar{1}2]$ and [101] zones (Fig. 4e). Dislocation walls are less common in the gabbro and the weakly deformed granodiorite but those observed occur along the [112], [101] and $[\bar{1}01]$ zones (Fig. 4d).

DISCUSSION

Marshall & McLaren (1977b) observed dislocation walls in plagioclase feldspars experimentally deformed at low to moderate strains. These dislocation walls were imaged with the TEM and had orientations approximately 15° from (001) and 15° from $(10\bar{1})$ consistent with dislocation wall orientations determined in this study. Debat *et al.* (1978) observed kink bands on the (001) and (110) planes and other simple crystallographic planes in plagioclase deformed at low temperatures suggesting that dislocation walls typically occur on or near simple crystallographic planes and are common in moderately deformed rocks.

Andrews (1984) observed that shear fractures are more abundant than extension fractures in naturally deformed plagioclase supporting a dislocation model for fracture formation in plagioclase. Two models of microcrack formation proposed by Stroh (1957) and Cottrell (1958) have commonly been observed in deformed metals and have been suggested as the mechanisms of fracturing in plagioclase (Mitra 1978). Stroh's (1957) model involves the pile-up of dislocations at an obstacle, often the grain boundary. At the boundary, stresses build up since dislocations cannot easily move past the boundary and may coalesce to form a microcrack. Microcracks formed in this manner occur at a relatively high angle to the dislocation pile-up. This does not satisfy the observations of microcracks and dislocation walls in plagioclase since the microcracks are typically observed along the dislocation walls (Fig. 2e).

In Cottrell's model (1958), leading dislocations from two intersecting dislocation bands coalesce to form a microcrack. In this case, microcrack orientation is at a moderate to high angle to the dislocation walls. This model may apply to some dislocation array intersections observed in plagioclase (Fig. 2a), although it does not readily explain the presence of microcracks along the dislocation walls (Fig. 2e).

A third model for crack nucleation has been proposed by Li (1961). This model involves the interaction of free dislocations with dislocations within a wall of dislocations. Long dislocation pile-ups are not required to produce a microcrack. Instead, dislocations at an angle to the wall can interact with dislocations in the wall at low stress and form a microcrack along the dislocation wall. Unlike the Stroh (1957) and Cottrell (1958) models, this model results in a stable microcrack which will not propagate since stresses do not build up as a result of a dislocation pile-up. Instead, these microcracks act as pre-existing flaws necessary for fracture propagation (Griffith 1921). This model is strongly supported by TEM observations of fractured plagioclase. Isolated dislocation walls with orientations similar to fracture planes observed in thin section are common in all plagioclase crystals examined. At the TEM scale, free dislocations are often observed to interact with dislocation walls. Under the proper diffracting conditions, tiny microcracks are observed along the dislocation wall where free dislocations interact with wall dislocations (Fig. 2e). These microcracks are elongated parallel to the wall as predicted in Li's (1961) model.

The similarity of orientations of fractures observed at the optical and TEM scales and dislocation walls in plagioclase of this study strongly supports a dislocation model for fracturing in plagioclase. Microcracks formed along dislocation walls or arrays act as nucleation sites for large-scale fractures and provide crystallographic control on fracture orientations.

Acknowledgements—The author wishes to acknowledge the financial support (NSF grant EAR 84-06070 and IGPP grant 1-443915-21817) and assistance provided by Dr H.-R. Wenk during the course of this work.

REFERENCES

Andrews, J. R. 1984. Fracture controlled feldspar shape fabrics in deformed quartzo-feldspathic rocks. *J. Struct. Geol.* **6**, 183–188.

Borg, I. & Heard, H. C. 1969. Mechanical twinning and slip in experimentally deformed plagioclases. *Contrib. Mineral. Petrol.* **23**, 128–135.

Brown, W. L. & Macaudiere, J. 1984. Microfracturing in relation to atomic structure of plagioclase from a deformed meta-anorthosite. *J. Struct. Geol.* **6**, 579–586.

Burri, C., Parker, R. L. and Wenk, E. 1967. *Die optische Orientierung der Plagioklase.* Birkhauser, Basel.

Cottrell, A. H. 1958. Theory of brittle fracture in steel and similar metals. *Trans. metall. Soc.* **223**, 192–203.

Debat, P., Soula, J. C., Kubin, L. & Vidal, J. L. 1978. Optical studies of natural deformation microstructures in feldspars (gneisses and pegmatites from Occitania, southern France). *Lithos* **11**, 133–145.

Griffith, A. A. 1921. The phenomenon of rupture and flow in solids. *Phil. Trans. R. Soc. Lond.* **221**, 163–197.

Li, J. C. M. 1961. High angle boundary—a dislocation core model. *J. appl. Phys.* **32**, 525–541.

Marshall, D. B. & McLaren, A. C. 1977a. Deformation mechanisms in experimentally deformed plagioclase feldspars. *Phys. Chem. Miner.* **1**, 350–370.

Marshall, D. B. & McLaren, A. C. 1977b. The direct observation and analysis of dislocations in experimentally deformed plagioclase feldspars. *J. Mater. Sci.* **12**, 893–903.

Mirams, R. C. 1964. The geology of the Mann Four Mile Sheet. Australian Department of Mines, Report of Investigations 25.

Mitra, G. 1978. Ductile deformation zones and mylonites. *Am. J. Sci.* **278**, 1057–1084.

Stroh, A. N. 1957. A thoery of the fracturing of metals. *Adv. Phys.* **57**, 418–465.

Theodore, T. G. 1970. Petrogenesis of mylonites of high metamorphic grade in the Peninsula Ranges of Southern California. *Bull. geol. Soc. Am.* **81**, 435–450.

Tullis, J. & Yund, R. 1987. Transition from cataclastic flow to dislocation creep of feldspar: mechanisms and microstructures. *Geology* **15**, 606–609.